Viscoelastic Properties of a Gum Vulcanizate at Large Static Deformations

J. L. SULLIVAN, *Engineering and Research Staff, Ford Motor Company, Dearborn, Michigan 48121*

Synopsis

The loss tangent corresponding to small sinusoidal oscillations superposed on a large static deformation is found to decrease with increasing static deformation ratio for a natural rubber gum vulcanizate. Further, the response functions of the stress–relaxation and the incremental stress–relaxation vs. time and the storage modulus vs. frequency are found not to be separable functions of time and strain effects. These findings are shown to indicate that the elastic contribution to the viscoelastic response of this elastomer increases more rapidly with the static deformation than does the relaxation contribution. The loss modulus, however, is found to be a separable function of time and strain effects. Hence, only one relaxation function is needed in the viscoelastic constitutive theory applied to this elastomer. The finite linear viscoelasticity theory as modified by Morman has a form which can account for these results. Predictions of the incremental stress–relaxation function from dynamic data are within 1% of experimental values.

INTRODUCTION

The storage and loss moduli, corresponding to small sinusoidal oscillations superposed on a large static strain, are in general found to be functions of the frequency, the dynamic strain amplitude, and the static prestrain. Studies on a variety of gum elastomers[1,2] indicate that the effects of the dynamic strain amplitude on the storage and loss moduli are negligible, but are quite pronounced for elastomers containing structured carbon blacks.[2–6] For the latter, the magnitude of this effect increases with the amount of added filler. Interest in the dynamic properties of elastomers corresponding to small sinusoidal oscillations superposed on large static deformations has increased.[1,6–8] Although initial studies using wave propagation techniques[9,10] were confined to the low dynamic strain amplitude, high frequency domain (1000 Hz), the increased refinement of forced nonresonant servohydraulic testing machines has permitted the investigation of the dynamic properties of prestrained elastomers in the frequency and dynamic strain amplitude ranges more typical of the conditions encountered in many engineering applications of elastomers (strain amplitudes from 0.005 to 0.05 and frequencies from 0.05 to 100 Hz).

In a previous report on a carbon-black-filled natural rubber compound,[6] the storage modulus was shown to demonstrate a separability of time, static deformation, and dynamic strain amplitude effects. However, in addition to an expected dynamic strain amplitude dependence,[2] the loss tangent was observed to be a function of the static deformation. This has also been shown for a filled SBR elastomer.[8] A static deformational dependence of the loss tangent indicates that the deformational dependences of the storage and loss moduli are different. Different deformational dependences for these moduli are inconsistent with many

Journal of Applied Polymer Science, Vol. 28, 1993–2003 (1983)
 CCC 0021-8995/83/061993-11$02.10

viscoelasticity theories, where it is assumed that the deformational dependences of the elastic and relaxation terms in the constitutive equation are the same.

In a previous report[1] on the natural rubber gum vulcanizate studied here, the stress–relaxation and the dynamic mechanical functions were concluded to demonstrate a separability of time and strain effects. However, in the paragraphs below it will be shown that, although this is true to good approximation, in reality the stress–relaxation, the storage modulus, and the incremental stress–relaxation functions are not separable functions of time and strain. The loss modulus, though, will be shown to be a separable function of these effects. For the strain fields of simple tension and pure shear, a set of stress–relaxation data to times as short as 0.2 s and dynamic data over a broad frequency range for all prestrains permits a more refined determination of material properties than was presented before. Also, the implications of these results in regard to the form of the viscoelastic constitutive theory required to characterize our elastomer is discussed.

THEORY

For the conditions of small relative motion superposed on a large static strain, the incremental true stress tensor according to the finite linear viscoelasticity theory of Coleman and Noll[11] as modified by Morman[12] can be written

$$\Delta\overset{\nabla}{\underset{\sim}{\sigma}}(t) = -\Delta p(t)\underset{\sim}{\mathbf{I}} + \underset{\approx}{\Omega}(\underset{\sim}{\mathbf{B}}_0)\{\underset{\sim}{\epsilon}(t)\} + 2\underset{\approx}{\Gamma}(\underset{\sim}{\mathbf{B}}_0)\int_0^\infty q(t-s)\dot{\underset{\sim}{\epsilon}}(s)\,ds \qquad (1)$$

where $\Delta\overset{\nabla}{\underset{\sim}{\sigma}}(t)$ is the Jaumann stress increment defined as

$$\Delta\overset{\nabla}{\underset{\sim}{\sigma}}(t) = \underset{\sim}{\sigma}(t) - \underset{\sim}{\sigma}_e + \underset{\sim}{\sigma}_e\underset{\sim}{\mathbf{W}} - \underset{\sim}{\mathbf{W}}\underset{\sim}{\sigma}_e \qquad (2)$$

The quantities $\underset{\sim}{\mathbf{I}}$, $\underset{\sim}{\mathbf{B}}_0$, and $\underset{\sim}{\epsilon}_0$ are the identity, static deformation (Finger's), and the small strain tensors, respectively. The fourth rank elasticity and relaxation tensors, $\underset{\approx}{\Omega}$ and Γ, respectively, are written as a function of the static deformation $\underset{\sim}{\mathbf{B}}_0$. The term $\Delta p(t)$ is the time-dependent pressure, $\underset{\sim}{\sigma}_e$ is the equilibrium true stress tensor, $\underset{\sim}{\mathbf{W}}$ is the infinitesimal rotation tensor corresponding to the small incremental strain, and t and s are the present and past times, respectively. The function $g(t)$ is a scalar relaxation function.[1,12] To obtain eq. (1) from the finite linear viscoelasticity theory, it has been assumed that the material relaxation spectrum, $H(\tau)$, is a separable function of time and strain effects.[12] Hence, the static deformational dependence appears outside the convolution integral in eq. (1). Also note that because carbon-black-filled elastomers demonstrate a dynamic strain amplitude dependence, the modified finite linear viscoelasticity theory[12] cannot be used to characterize such systems. This is a consequence of the fact the only linear terms in the small amplitude strain were retained in eq. (1).

Of special interest here is the strain history of small relative motion superposed on a large static strain. For uniaxial extension, the deformation ratio for this history is

$$\lambda(t) = \lambda[l + \epsilon(t)] \qquad (3)$$

where

$$\lambda = l/l_0 \qquad (4)$$

and

$$\epsilon(t) = d(t)/l \tag{5}$$

In eqs. (3)–(5), $\epsilon(t)$ is the true strain, l_0 and l are the undeformed and deformed specimen dimensions, respectively, λ is the static deformation ratio, and $d(t)$ is the small displacement motion.

When specialized to the above history, eq. (1) yields the following:

$$E(t) = E_e(\lambda) + \hat{\Gamma}(\lambda)g(t) \tag{6}$$

for a small superposed step in strain, and

$$E_1 = E_e(\lambda) + \hat{\Gamma}(\lambda)G_s(\omega) \tag{7}$$

and

$$E_2 = \hat{\Gamma}(\lambda)G_c(\omega) \tag{8}$$

for small superposed sinusoidal oscillations. The frequency dependent functions appearing in eqs. (7) and (8) are

$$G_s(\omega) = \omega \int_0^\infty g(t) \sin \omega t \, dt \tag{9}$$

and

$$G_c(\omega) = \omega \int_0^\infty g(t) \cos \omega t \, dt \tag{10}$$

where ω ($= 2\pi\nu$) is the angular frequency. Equations (7) and (8) are the storage and loss moduli, respectively. Equation (6) is the relaxation modulus and it is a function of the static state of strain. The equilibrium modulus is defined as

$$E_e = \lambda \, d\sigma_e/d\lambda \tag{11}$$

when σ_e is the equilibrium true stress. For stress–relaxation corresponding to a large step in strain, the modified FLV theory yields[1,12]

$$\sigma(t) = \sigma_e(\lambda) + \Gamma(\lambda)g(t) \tag{12}$$

The deformational dependences of the relaxation terms appearing in eqs. (6)–(8) and (12) are related as follows:

$$\hat{\Gamma}(\lambda) = \lambda \, d\Gamma/d\lambda \tag{13}$$

This results from the linearization of eq. (1) for small relative motion in uniaxial extension.

EXPERIMENTAL

The elastomer system reported herein is a natural rubber gum vulcanizate; details of the recipe appear elsewhere.[1] The tests were conducted with the following strain history. For stress–relaxation tests corresponding to large steps in strain, the specimen was deformed to a predetermined deformation ratio (λ) in 50 ms, and stress–relaxation data was collected up to 2000 s. It is assumed that essentially all of the relaxation is complete within 2000 s. After the step

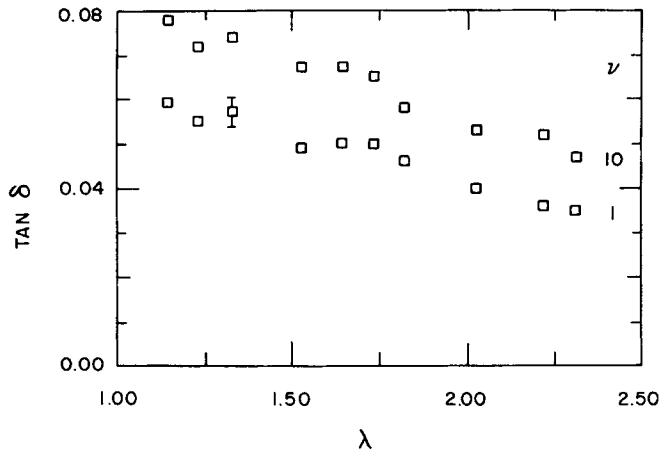

Fig. 1. The material loss tangent vs. λ for the frequencies of 1 and 10 Hz.

stress–relaxation test was complete, a small step in strain was superposed. Data was collected up to 2000 s. The amplitude of the small step in strain was calculated from eq. (5) and the condition $d(t) = d$ (a constant) for all $t > 0$. For the tests reported here, ϵ is equal to 0.02. From the small step stress–relaxation data, the relaxation modulus at each λ is calculated from

$$E(t) = \lambda \Delta P(t)/(A_0 \epsilon_0) + \sigma_e \tag{14}$$

where $\Delta P(t)$ is the incremental load relaxation with time, A_0 is the undeformed cross-sectional area, and σ_e is the equilibrium true stress, taken to be σ (2000).

After the small step relaxation test was complete, the overall deformation was returned to λ, and the system was allowed to relax for 10 min. Then small sinusoidal oscillations of varying frequency at a strain amplitude of 0.02 were superposed on the static deflection λ according to eq. (5), where

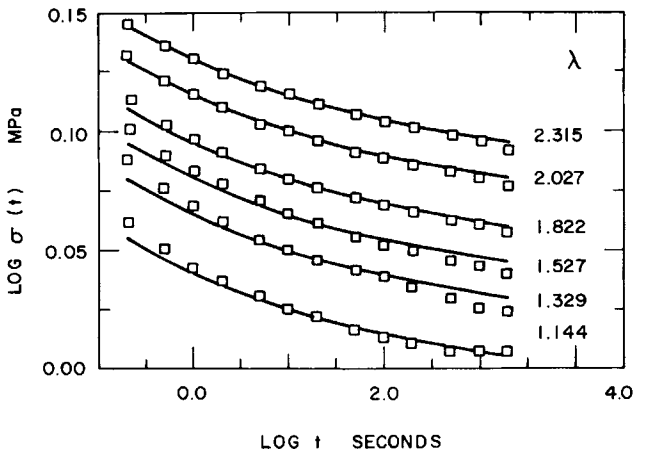

Fig. 2. Stress–relaxation data in pure shear for the deformation ratios indicated at the right. In order to facilitate comparison, a single reference curve has been drawn through each data set.

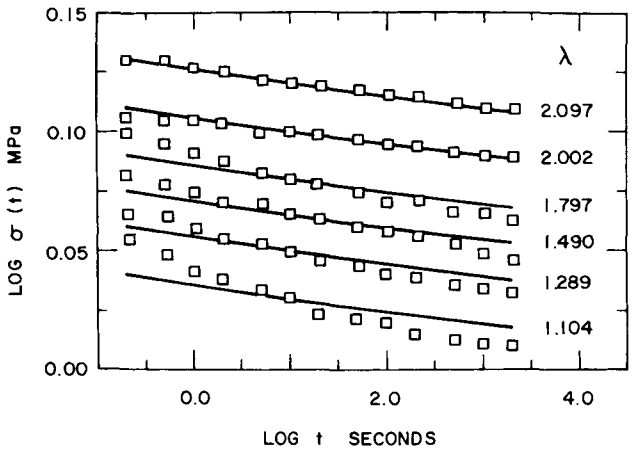

Fig. 3. Stress-relaxation data in simple tension for the deformation ratios indicated at the right. In order to facilitate comparison, a single reference curve has been drawn through each data set.

$$d(t) = d_0 \sin \omega t \tag{15}$$

Hence, the strain amplitude is

$$\epsilon_0 = d_0/l \tag{16}$$

The tests were conducted at increasing frequencies, where approximately 30 s elapsed at zero oscillation before the next frequency was applied. The storage and loss moduli were calculated from the data using the following equations, respectively[7]:

$$E_1 = \lambda \Delta P/(A_0 \epsilon_0) \cos \delta + \sigma_e \tag{17}$$

and

$$E_2 = \lambda \Delta P/(A_0 \epsilon_0) \sin \delta \tag{18}$$

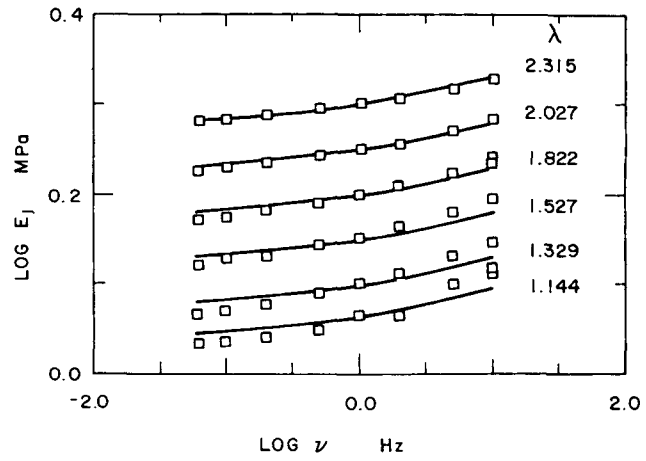

Fig. 4. Storage modulus vs. frequency data in pure shear for the prestrains indicated at the right. In order to facilitate comparison, a single reference curve has been drawn through each data set.

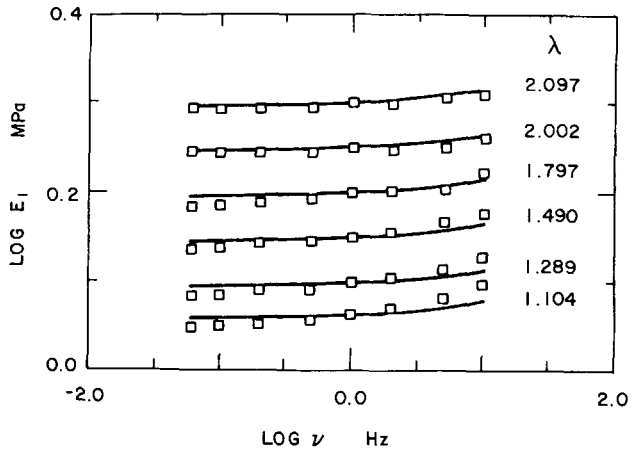

Fig. 5. Storage modulus vs. frequency data in simple tension for the deformation ratios indicated at the right. In order to facilitate comparison, a single reference curve has been drawn through each data set.

where ΔP is the load sine wave amplitude and δ is the phase angle between the load and the stroke. Tests were conducted in pure shear and simple tension at $T = 30° \pm 1°C$. Details about the test equipment and the procedures necessary to reduce noise and to correct for load vs. stroke phase angle errors appear elsewhere.[1,6]

RESULTS AND DISCUSSION

The deformation functions for the elastic and relaxation terms in eq. (12) must be equal to zero at $\lambda = 1$. However, in general these functions need not be the same. For a material for which they are not the same, the loss tangent (E_2/E_1), which is the ratio of eq. (8) to eq. (7), would be a function of λ. As seen in Figure

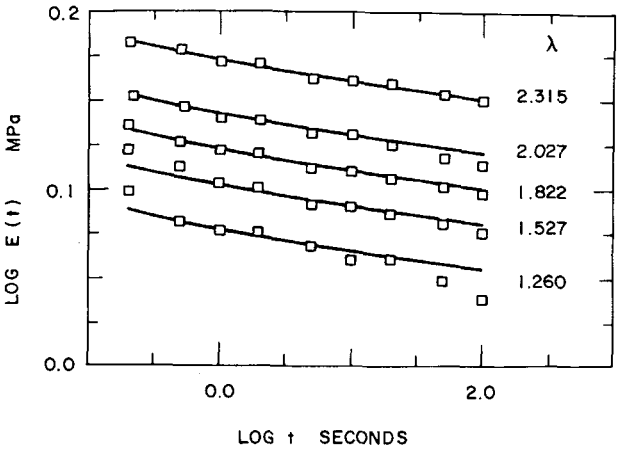

Fig. 6. Incremental relaxation modulus data in pure shear for the deformation ratios indicated at the right. In order to facilitate comparison, a single reference curve has been drawn through each data set.

1, our gum elastomer shows a pronounced prestrain dependence for the loss tangent (tan ϕ). These data represent frequencies of 1 and 10 Hz, and the error typical of the measurements is shown by the error bar in the figure. Another manifestation of different deformational dependences for the relaxation and elastic terms is seen in Figures 2–6. In each figure, a single reference curve has been drawn through each data set. This was done in order to facilitate a comparison of the response functions as a function of the prestrain. In all the plots (Figs. 2–6), it is observed that the time rate of change of the response functions log $\sigma(t)$ and log $E(t)$, and the frequency rate of change of log E_1 decreases with increasing λ. As seen in the figures, decreases in the slopes of response function curves with increasing λ occur in the time and frequency domains for both simple tension and pure shear. These decreases demonstrate that the elastic deformational functions appearing in eqs. (6), (7), and (12) increase more rapidly with λ than the corresponding relaxation deformational dependences. This is consistent with the decrease of the loss tangent with increasing static deformation.

A more quantitative indication that the time rate of change of log $\sigma(t)$ decreases with increasing λ is seen in Figure 7 for stress relaxation results. The figure is a plot of $d \log \sigma(t)/dt$ at $t = 1$ s vs. λ for two pure shear specimens and one simple tension specimen. These data show a consistent decreasing trend of the inverse relaxation time with increasing λ. The simple tension data are somewhat more scattered than the pure shear results, but this is due to an inherently lower signal to noise ratio for simple tension tests. The inverse relaxation times at 1 s were calculated from

$$-d \log \sigma(t)/dt = Am/(A + B) \tag{19}$$

where the constants A, B, and m were obtained from a nonlinear least squares fit of the function

$$\sigma(t) = At^{-m} + B \tag{20}$$

to the relaxation data at each λ. B was allowed to vary in such a way as to maximize the coefficient of determination corresponding to a linear least squares

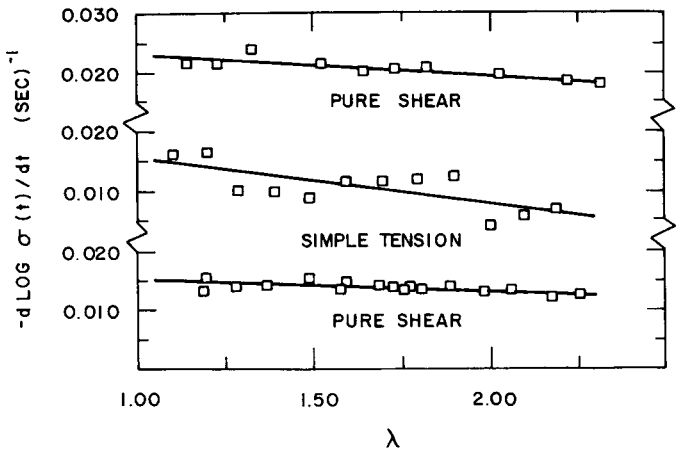

Fig. 7. The time rate of changes of the log $\sigma(t)$ vs. λ for two pure shear specimens and one simple tension specimen.

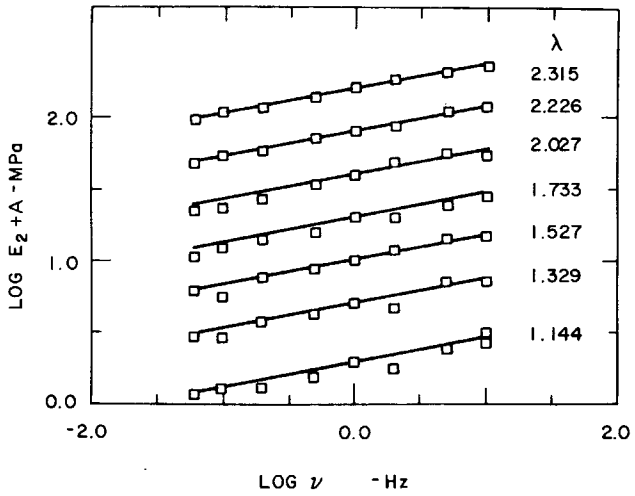

Fig. 8. The loss modulus vs. frequency in pure shear for the deformation ratios indicated at the right. In order to facilitate comparison, a single reference curve has been drawn through each data set. The shift factors (A) are from bottom to top: 1.433, 1.834, 2.138, 2.360, 2.656, 2.950, and 3.232.

fit of $\log[\sigma(t) - B]$ vs. $\log t$. Values of this coefficient were typically 0.99, indicating an excellent fit of the data.

An inspection of the loss modulus data seen in Figure 8 reveals a linear dependence of $\log E_2$ with $\log \nu$. All of the data, despite the prestrain, are fit well by a single reference curve. This shows that E_2 is a separable function of time and strain effects. Consequently, eq. (8) with its single relaxation function is a perfectly adequate representation of loss modulus data. Further, these loss modulus results show that the relaxation spectrum is also a separable function of time and strain effects.

Some other viscoelasticity theories express the loss modulus as the sum of products of deformation functions and relaxation functions.[7,13] When these theories are applied to our results, all nontrivial relaxation functions must be identical.

A good test of the suitability of any viscoelasticity theory is whether or not data from one strain history can be used to predict results in another history. A comparison of prediction vs. experiment for incremental stress–relaxation corresponding to small relative motion superposed on a large statically relaxed deformation appears in Figure 9. The incremental relaxation modulus data has been compared to theoretical relaxation modulus predictions based on dynamic data using the Schwartzl approximation[14]:

$$E(t) = E_1(\omega) - 0.566E_2(\omega/2) + 0.203E_2(\omega) \tag{21}$$

where $t = 1/\omega$. The predicted curves had to be shifted by approximately 1% to superpose with the data, but this is certainly within the precision of the measurements. Note that the theory curve based on the dynamic data for $\lambda = 1.329$ is steeper than a similar curve based on $\lambda = 2.315$ data and does not fit the $E(t)$ vs. t data for the larger λ's. Although our lowest frequency is approximately 0.06 Hz (corresponding to $t \simeq 2.5$ s) the overlap of the curves and the data for a given value of λ is excellent up to 100 s. These results show that a single in-

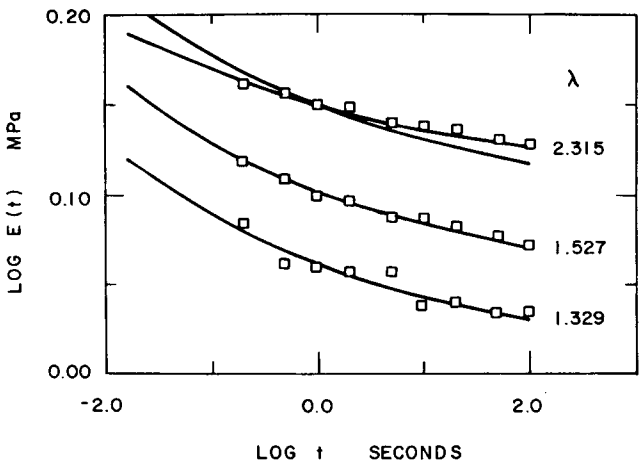

Fig. 9. Incremental relaxation modulus data (■) and theoretical predictions (—) in pure shear for the deformations indicated at the right. The steeper curve fitted through all the data is based on dynamic data for $\lambda = 1.329$ and the more gradual curve fitted to the $\lambda = 2.315$ data is based on dynamic data for that deformation.

tegral constitutive theory characterizes our system. The storage and loss moduli data used to calculate the $E(t)$ curves in Figure 9 was first smoothed to the functions, respectively,

$$E_1 = A\nu^m + B \tag{22}$$

and

$$E_2 = C\nu^n \tag{23}$$

Unlike the results presented above, it was reported before[1] for the same elastomer compound that the $\sigma(t)$ vs. t and the E_1 vs. ν behaviors demonstrated a separability of time and strain effects. However, in that report the stress–relaxation data did not go to as short a time, and the dynamic data did not cover a fixed frequency range for all predeformations as is characteristic of the corresponding data in this report. Further, those tests were performed exclusively in simple tension, a deformation state more troubled with noise problems when experiments are conducted on large servohydraulic test machines. Nevertheless, the assumption of a separability of time and strain effects made in Ref. 1 is a good approximation for those data because predicted and experimental E_1 values agreed to within 11%.

Although the time dependence of the incremental relaxation modulus and the frequency dependence of the storage modulus show a distinct static prestrain dependence, the magnitude of the departures from separable behavior is comparatively small. For example, if separable behavior is assumed, an error of approximately 8% is introduced into a prediction of E_1 in pure shear for $\lambda = 2.315$ when E_1 for $\lambda = 1.144$ is simply scaled up by a factor proportional to the ratio of the elastic moduli at these two deformations. From an engineering point of view, this error is acceptable. However, such an error will increase as the frequency increases or the relative magnitude of the relaxation component of a material increases. In fact, we have unpublished data for a carbon-black-filled

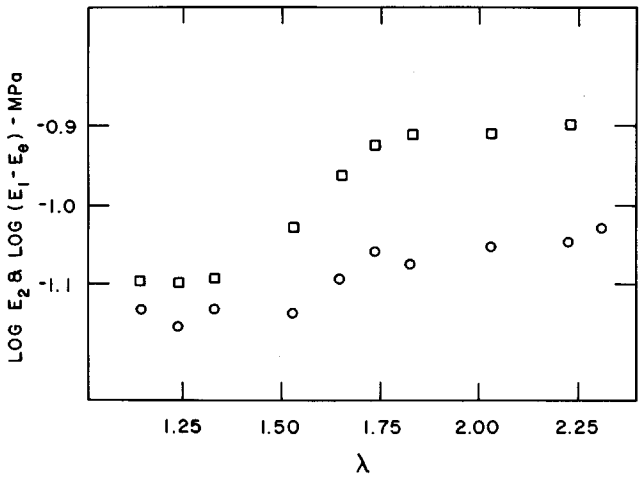

Fig. 10. The loss modulus (●) and the relaxation component of the storage modulus (□) vs. the static deformation at 1 Hz.

butyl elastomer where the separability assumption would introduce an error of 17% over a static prestrain range of $\lambda = 1.1$–2.1.

In Figure 10 appears a plot of the log of E_2 and $E_1 - E_e$ (λ) vs. λ. The latter quantity is the relaxation component of the storage modulus. The data show that both $E_1 - E_e$ and E_2 first increase and then tend to level off with increasing λ. The quantity $E_1 - E_e$ was calculated from E_1 data and from smoothed $E(t)$ vs. λ data at $t = 2000$ s for E_e. However, because $E_1 - E_e$ is approximately an order of magnitude smaller than either of its components, the typical 5% errors in E_e can result in errors approaching 50% for the relaxation component of the storage modulus. So the plot of $E_1 - E_e$ vs. λ must be viewed at best as qualitative. Actually, the most reliable indication that the deformational dependence of the relaxation components of eqs. (6)–(8), and (12) are different than the corresponding elastic components is the change in the slopes of response function curves on log vs. log scales for a given t or ν with changes in the prestrain. This has been shown above in Figures 2–6.

CONCLUSION

The viscoelastic properties of a natural rubber gum vulcanizate for various levels of prestrain have been studied. The loss tangent is found to decrease with increasing static deformation ratio. Changes in the slopes of stress–relaxation, incremental stress–relaxation curves, and storage modulus vs. frequency curves with changes in prestrain are consistent with the deformational dependence of the loss tangent; further analysis shows that the deformational dependence of the relaxation term in single integral theories increases more slowly with the static deformation than the elastic term. The storage modulus, stress–relaxation, and incremental stress–relaxation behaviors are not separable functions of time and strain effects. However, the loss modulus is a separable function of these effects. This shows that only a single relaxation function is needed for a viscoelastic characterization of our system.

Predictions of the incremental relaxation modulus from dynamic data agree

with experiment values to within 1%. This agreement, which is found for all prestrain levels, shows that a single integral constitutive theory, such as the FLV theory modified by Morman, can characterize the viscoelastic properties of our gum vulcanizate.

References

1. J. L. Sullivan, K. N. Morman, and R. A. Pett, *Rubber Chem. Technol.*, **53,** 805 (1980).
2. A. R. Payne and R. E. Whittaker, *Rubber Chem. Technol.*, **44,** 440 (1971).
3. A. I. Medalia, *Rubber Chem. Technol.*, **46,** 877 (1973).
4. A. Voet and W. N. Whitaker, Jr., *Rubber World*, **146** (3), 77 (1962).
5. A. Voet and F. R. Cook, *Rubber Chem. Technol.*, **41,** 1207 (1968).
6. J. L. Sullivan and V. C. Demery, *J. Polym. Sci., Polym. Phys. Ed.*, **20,** 2083 (1982).
7. W. Goldberg and G. Lianis, *J. Appl. Mech.*, **35,** 433 (1968).
8. E. A. Meinecke and S. Maksin, *Rubber Chem. Technol.*, **54,** 857 (1981).
9. P. Mason, *J. Appl. Polym. Sci.*, **1,** 212 (1960).
10. P. Mason, *J. Appl. Polym. Sci.*, **1,** 63 (1960).
11. B. D. Coleman and W. Noll, *Rev. Mod. Phys.*, **33,** 239 (1961).
12. K. N. Morman, Jr., Ford Technical Report on the Application of The Finite Linear Viscoelasticity Theory to Incompressible Materials Exhibiting Separability of Time and Strain Effects, *J. Rheol.*, to appear.
13. B. Bernstein, E. A. Kearsley, and L. J. Zapas, *Trans. Soc. Rheol.*, **VII,** 391 (1963).
14. F. R. Schwartzl, *Deformation and Fracture of High Polymers*, H. H. Kausch, J. A. Hassell, and R. I. Jaffee, Eds., Plenum, New York, London, 1973.

Received July 13, 1982
Accepted January 19, 1983